

Growing a Twig to Accelerate Large Vision-Language Models

Zhenwei Shao^{1*} Mingyang Wang^{1*} Zhou Yu^{2†} Wenwen Pan¹ Yan Yang¹
Tao Wei² Hongyuan Zhang² Ning Mao² Wei Chen² Jun Yu³

¹ School of Computer Science, Hangzhou Dianzi University, China ²Li Auto Inc., China

³School of Intelligence Science and Engineering, Harbin Institute of Technology (Shenzhen), China

{shaozw, kaka.my, yuz, yangyan, panww}@hdu.edu.cn,

{weitao, zhanghongyuan, maoning, chenwei10}@lixiang.com, yujun@hit.edu.cn

Abstract

Large vision-language models (VLMs) have demonstrated remarkable capabilities in open-world multimodal understanding, yet their high computational overheads pose great challenges for practical deployment. Some recent works have proposed methods to accelerate VLMs by pruning redundant visual tokens guided by the attention maps of VLM’s early layers. Despite the success of these token pruning methods, they still suffer from two major shortcomings: (i) considerable accuracy drop due to insensitive attention signals in early layers, and (ii) limited speedup when generating long responses (e.g., 30 tokens). To address the limitations above, we present TwigVLM—a simple and general architecture by “growing” a lightweight twig upon an early layer of the base VLM. Compared with most existing VLM acceleration methods purely based on visual token pruning, our TwigVLM not only achieves **better accuracy retention** by employing a twig-guided token pruning (TTP) strategy, but also yields **higher generation speed** by utilizing a self-speculative decoding (SSD) strategy. Taking LLaVA-1.5-7B as the base VLM, experimental results show that TwigVLM preserves 96% of the original performance after pruning 88.9% of visual tokens and achieves 154% speedup in generating long responses, delivering significantly better performance in terms of both accuracy and speed over the state-of-the-art VLM acceleration methods. Code will be made publicly available.

1. Introduction

The revolution in large language models (LLMs) has fundamentally reshaped the landscape of artificial intelligence [4, 17, 44]. Meanwhile, there has been growing interest in building large vision-language models (VLMs) [1, 9, 25,

*Work done during an internship at Li Auto Inc.

†Zhou Yu is the corresponding author.

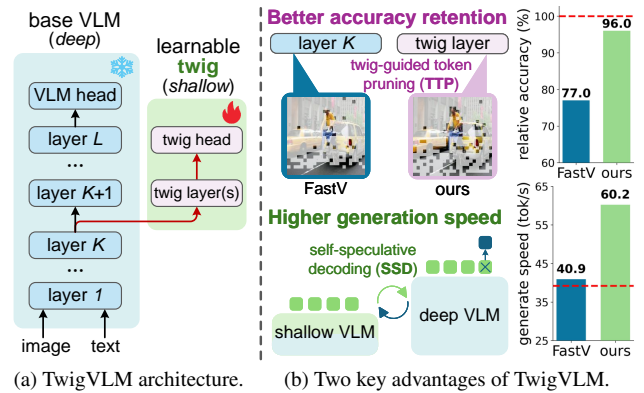


Figure 1. **Our TwigVLM overview.** (a) Given a base deep VLM, the TwigVLM is obtained by freezing the whole VLM while training a shallow twig block upon an early layer of the VLM. (b) Compared to the VLM acceleration methods based on visual token pruning (e.g., FastV [8]), TwigVLM not only achieves better accuracy retention by employing a twig-guided token pruning (TTP) strategy, but also yields higher generation speed by utilizing a self-speculative decoding (SSD) strategy [12]. Both FastV and TwigVLM take LLaVA-1.5-7B [30] as the base VLM (red dotted lines in the bar graphs) with the same pruning ratio of 88.9%.

29, 39, 53, 68], which can perform general-purpose visual understanding and reasoning and be used in a wide range of tasks such as object grounding [36, 40], document understanding [35, 54], GUI controlling [47, 60], and robotics [3, 22]. Despite the remarkable progress achieved by these large VLMs, they are usually parametric-intensive and computational-heavy. This poses great challenges for using these models in computation-constrained platforms or low-latency scenarios. Therefore, the research on VLM acceleration is of practical and emergent demands.

As the computational cost of the transformer architecture [46] increase quadratically with the length of token sequence, an effective way to accelerate VLMs is to reduce the length of tokens. Moreover, visual tokens usually contain much more redundant information than textual tokens

[8], especially in high-resolution images and long videos. Therefore, a series of works on visual token pruning has been proposed [8, 32, 52, 62]. For instance, FastV [8] leverages attention signals from an early layer of the VLM to drop redundant tokens for subsequent layers. Many following works have extended FastV’s idea to progressive token reduction across layers via pruning and merging operations [32, 62], while some others have been proposed to use the attention maps from the visual encoder to guide the visual token pruning before being input into the VLM backbone [52, 61]. Despite the success they have achieved, they still suffer from the following two major shortcomings:

- (i) To effectively reduce computational costs, a large proportion of visual tokens are usually pruned in the early layers, which is guided by the attention map of the same layer. However, the attention signals in the early layers are insensitive to the task, which restricts the quality of retained visual tokens and leads to a considerable accuracy drop of the accelerated VLM.
- (ii) The VLM inference process consists of the prefilling and decoding stages. Most token pruning-based approaches only focus on the acceleration of the prefilling stage while paying less attention to the decoding stage, which is the most time-consuming part of the inference process. This results in a significant efficiency gap between the theoretical estimation and practical application, especially in the tasks that generate long responses (*e.g.*, more than 30 tokens).

We ask: *Is it possible to address the two limitations above in one unified framework?*

To this end, we present TwigVLM, a simple and general VLM acceleration approach by appending a lightweight *twig* block upon an early layer of the base VLM (see Figure 1a). After efficient post-training of the twig block only, the learned twig block is used in both the prefilling and decoding stages of inference. As shown in Figure 1b, our TwigVLM not only achieves better accuracy retention by employing a twig-guided token pruning (TTP) strategy, but also yields higher generation speed by utilizing a self-speculative decoding (SSD) strategy [12]. To summarize, the synergistic effect of the TTP and SSD strategies enables holistic inference acceleration of both the prefilling and decoding stages at maximum accuracy retention.

Extensive experiments on a wide range of VLM benchmarks validate the effectiveness of the proposed method. Without bells and whistles, TwigVLM preserves 96% of the original accuracy after pruning 88.9% of visual tokens and achieves 154% speedup in generating long responses. These results demonstrate significant improvements over previous state-of-the-art methods in terms of both accuracy and speed. Moreover, our study also discloses a new aspect for VLM acceleration, *i.e.*, long response generation, which is crucial in real-world scenarios.

2. Pilot Studies

Before introducing our TwigVLM, we conduct two pilot studies on the accuracy retention and generation speed, respectively, which reveals some crucial but easily overlooked observations in previous VLM acceleration works.

2.1. Preliminaries

To better understand the pilot studies, we first provide a concise overview of the architecture and two-stage inference process of modern VLMs. After that, we briefly introduce FastV [8], a typical VLM acceleration method via adaptive visual token pruning at inference.

VLM architecture and inference. Modern VLMs are usually comprised of a vision encoder and an LLM, where the LLM further consists of a stack of L transformer layers.

During inference, the learned VLM first encodes an input image as a sequence of M visual tokens $\mathbf{X}_v = [\mathbf{v}_1, \dots, \mathbf{v}_M] \in \mathbb{R}^{M \times d}$ and represents a language prompt as a sequence of N textual tokens $\mathbf{X}_q = [\mathbf{q}_1, \dots, \mathbf{q}_N] \in \mathbb{R}^{N \times d}$, where d is the common dimensionality of the multimodal tokens. These two groups of tokens are concatenated into $\mathbf{X} = [\mathbf{X}_v, \mathbf{X}_q]$, which is then passed through the LLM to generate a sequence of S response tokens $\mathbf{y} = (y_1, \dots, y_S)$ in an autoregressive manner. At each generation step j , we have:

$$y_j = \underset{\hat{y}_j}{\operatorname{argmax}} p_{\text{LLM}}(\hat{y}_j | \mathbf{X}, \mathbf{y}_{<j}), \quad (1)$$

where $\mathbf{y}_{<j}$ is the response sequence before the current token y_j . In practice, the iterative generation process is divided into the *prefilling* and *decoding* stages by leveraging the KV-cache technique [67].

Prefilling stage. This stage executes the forward pass of the input tokens \mathbf{X} , which remains unchanged during the response generation. Therefore, their intermediate representations in the LLM, namely the key-value pairs in each self-attention (SA) block of the transformer layer, can be cached and reused in the subsequent decoding stage. Specifically, the SA operation is given by:

$$\begin{aligned} \text{SA}(\mathbf{Q}, \mathbf{K}, \mathbf{V}) &= \mathbf{A}\mathbf{V} = \operatorname{softmax}(\mathcal{M}(\mathbf{Q}\mathbf{K}^T / \sqrt{d}))\mathbf{V} \\ \mathbf{Q} &= \mathbf{X}\mathbf{W}_q, \quad \mathbf{K} = \mathbf{X}\mathbf{W}_k, \quad \mathbf{V} = \mathbf{X}\mathbf{W}_v, \end{aligned} \quad (2)$$

where $\mathcal{M}(\cdot)$ is the causal masking function and \mathbf{A} is the attention map of query-key pairs. $\mathbf{Q}, \mathbf{K}, \mathbf{V}$ denote the queries, keys, and values, while $\mathbf{W}_q, \mathbf{W}_k, \mathbf{W}_v$ are their linear projection matrices, respectively.

As mentioned, the key-value pairs \mathbf{K} and \mathbf{V} of all transformer layers in the LLM are stored in the KV-cache to expedite the decoding stage.

Decoding stage. The generation of the response token y_j is based on its previous tokens $(\mathbf{X}, \mathbf{y}_{<j})$. As the attention

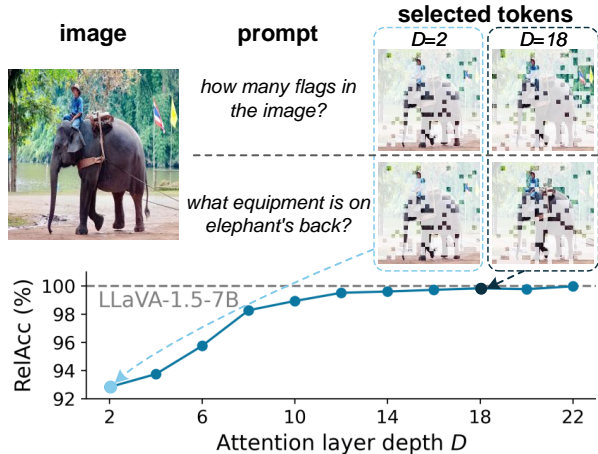


Figure 2. **Attention quality for token selection.** The RelAcc (defined in §4.2) is evaluated on GQA [19] and TextVQA [42], which measures the accuracy gap between LLaVA-1.5-7B and its FastV variants with $R=128$ and varied attention layer depth D . Taking an image with two prompts as an example, we visualize their attention maps from typical layers $D=2$ and 18, respectively.

computation in Eq.(2) is causal and parallel for each query, the generation for y_j can be accelerated by feeding only the *single* token into the LLM and computing its corresponding key and value, while reusing the rest key-value pairs from the KV-cache. After each decoding step, the computed key-value pairs for y_j are appended to the KV-cache for the efficient generation of subsequent tokens.

Visual token pruning. The visual tokens in VLMs are much more than the textual tokens and exhibit severe redundancy [32, 62]. To accelerate the inference process of VLMs, some recent works such as FastV [8] and Sparse-VLM [62] have been proposed to drop redundant visual tokens based on the attention scores during the prefilling stage. Specifically, FastV works by passing the input tokens \mathbf{X} through the first K VLM layers to obtain the attention map $\mathbf{A}^{(K)}$ and token sequence $\mathbf{X}^{(K)} = [\mathbf{X}_v^{(K)}, \mathbf{X}_q^{(K)}]$ after layer K . Denoting R as the number of visual tokens after pruning, the retained token sequence $\hat{\mathbf{X}}^{(K)}$ is obtained as follows:

$$\begin{aligned} \hat{\mathbf{X}}^{(K)} &= \mathcal{P}(\mathbf{X}^{(K)}, \mathbf{A}^{(K)}, R) \\ &= \left[\text{TopR} \left(\mathbf{X}_v^{(K)}, \sum_{i=M+1}^{M+N} \mathbf{A}^{(K)}[i, 1:M] \right), \mathbf{X}_q^{(K)} \right]. \end{aligned} \quad (3)$$

$\text{TopR}(\mathbf{X}_v^{(K)}, \mathbf{a})$ selects top- R most significant visual tokens from $\mathbf{X}_v^{(K)}$, which is guided by the attention scores \mathbf{a} from textual tokens to visual tokens. In FastV, both K and R are set to small values, which means the token lengths are short in most VLM layers, thus the computational complexity of the prefilling stage is significantly reduced at the expense of a certain amount of performance drop. For a fair compari-

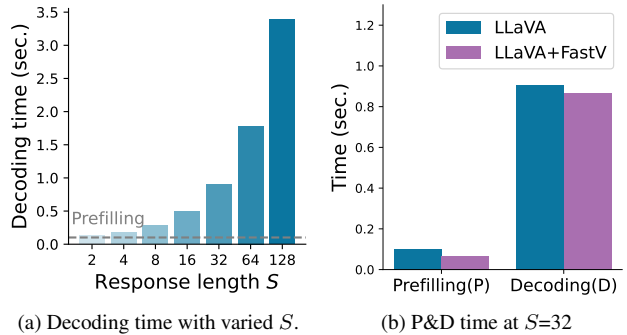


Figure 3. **Prefilling and decoding time costs.** (a) Prefilling time (gray dotted line) and decoding time for LLaVA-1.5-7B [30] with different response lengths. (b) Prefilling (P) and decoding (D) time comparisons of LLaVA-1.5-7B and its FastV-based variant.

son of different token pruning methods, the average number of retained tokens \bar{R} is used and defined as follows¹:

$$\bar{R} = [M \times K + R \times (L - K)]/L \quad (4)$$

2.2. Study 1: Attention Quality for Token Selection

The performance of visual token pruning methods heavily depends on the quality of the chosen attention map for pruning. Existing approaches often utilize the attention map from an early layer, *e.g.*, $K=2$, to guide the visual token pruning at the same layer. We ask: *Whether an attention map from a late layer contains more informative signals to facilitate token pruning?* Notably, directly applying the attention map of a late layer to guide the token pruning at an early layer will inevitably introduce redundant computation, this pilot study only aims to evaluate the quality of the attention maps in different layers.

The pilot experiment is conducted as follows. We use LLaVA-1.5-7B as the base VLM and FastV as the token pruning strategy. Different from the original FastV that selects and prunes visual tokens at the same layer K , we perform token selection guided by the attention of the D -th layer and then perform token pruning at the K -th layer. In this experiment, we set $K=2$ and let $D \geq K$. From the results in Figure 2, we can see that the accuracy grows as the attention depth D increases, showing that the attention maps from later layers provide more precise signals for visual token pruning than those from early layers. We hypothesize that later layers are closer to the prediction head (*i.e.*, the loss function), thus their attention maps understand the relation between multimodal tokens more accurately. Moreover, from the visualized attention maps, we find that the selected tokens by early-layer attention ($D=2$) are insensitive to different prompts, while the selected tokens by late-layer attention ($D=18$) are more related to the prompt. This observation also verifies our hypothesis above.

¹The computed result will be rounded to the nearest integer.

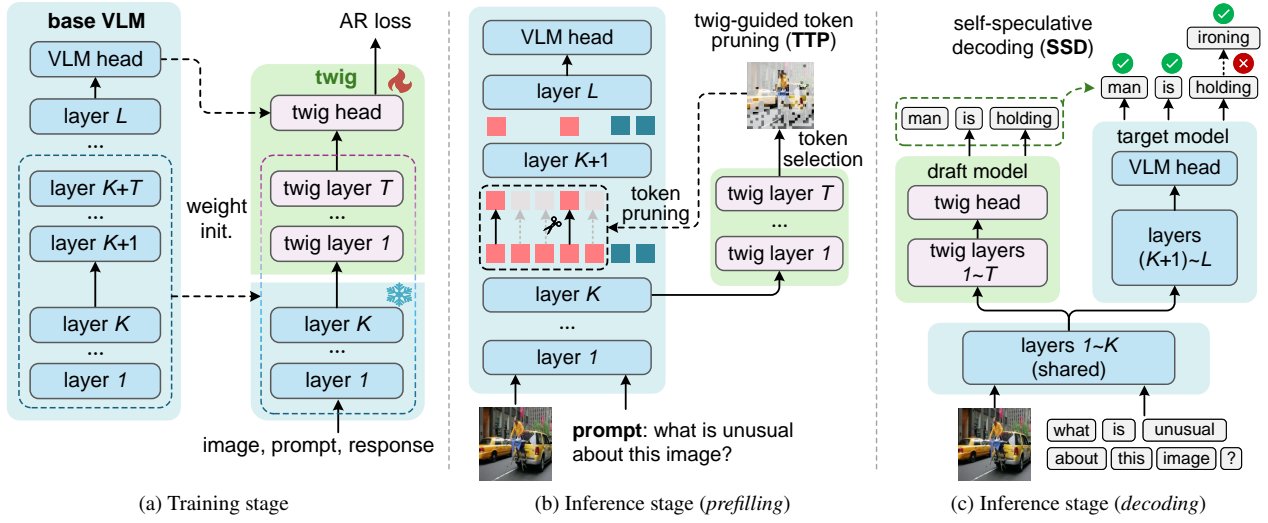


Figure 4. **Training and two-stage inference of TwigVLM.** (a) The twig block is initialized from the base VLM and is coupled with the first K layers of base VLM to form a shallow model, which can be trained efficiently. (b) In the prefilling stage, different from previous approaches that perform token selection based on the attention maps from the base VLM, TwigVLM introduces a twig-guided token pruning (TTP) strategy to obtain more precise signals to guide the pruning of visual tokens. (c) In the decoding stage, the shallow and deep sub-networks act as the draft and target models respectively, enabling it to perform the self-speculative decoding (SSD) [12] to accelerate the generation of long responses.

2.3. Study 2: Prefilling and Decoding Time Costs

As mentioned above, the inference process consists of the prefilling and decoding stages. FastV and other token-pruning methods primarily accelerate the prefilling stage. We ask: *Can these methods also facilitate the acceleration of the decoding stage, especially when the generated response is relatively long?* This is a practical question since VLMs are often expected to generate long responses (e.g., 30 tokens) in real-world scenarios.

To answer this question, we conduct the pilot experiment as follows. We take LLaVA-1.5-7B [30] as the base VLM and compute its time spent on the prefilling and decoding stages for the response length S ranging from 2 to 128. The results in Figure 3a show a linear increase in decoding time w.r.t. the response length S , while the prefilling time can be neglected when $S \geq 32$.

Next, we compare the prefilling and decoding times of LLaVA-1.5-7B and its FastV-based variant (LLaVA+FastV) when generating responses of the same length $S=32$. From Figure 3b, we observe that although FastV effectively reduce the prefilling time, it attains limited speedup in the decoding stage. This frustrating observation can be explained by two facts: (i) the KV-cache mechanism undermines the speedup for SA blocks achieved by FastV, and (ii) FastV does not accelerate the FFN blocks during decoding, but they account for the majority of the computational costs.

To summarize, these observations highlight the significance and necessity of improving the decoding efficiency for long response generation.

3. The Proposed TwigVLM

Inspired by the pilot studies above, we propose TwigVLM, a simple yet effective approach for accelerating VLMs. As depicted in Figure 4, our TwigVLM is obtained by training a lightweight twig block upon an early layer of a frozen VLM. Subsequently, the learned twig block is used in both the prefilling and decoding stages to simultaneously achieve more precise visual token pruning and faster generation speed for long responses.

3.1. Architecture and Training of TwigVLM

Denoting a L -layer base VLM as $\mathcal{M}_b = \{\mathcal{T}_l\}_{l=1}^L$, we attach a twig block $\{\mathcal{G}_t\}_{t=1}^T$, i.e., an extra lightweight module with T transformer layer, upon an early layer of \mathcal{M}_b . Specifically, the twig block is appended after the K -th layer \mathcal{T}_K , resembling a twig growing from a tree trunk. When $K + T \ll L$, we obtain a very shallow VLM by combining the twig block and its based K trunk layers $\mathcal{M}_s = \{\mathcal{T}_k\}_{k=1}^K \cup \{\mathcal{G}_t\}_{t=1}^T$.²

As shown in Figure 4a, the training strategy of TwigVLM is simple yet efficient. All the model weights in the twig block are initialized from the layers $\{\mathcal{T}_i\}_{i=K+1}^{K+T}$ and the prediction head of \mathcal{M}_b , respectively. After that, the shallow VLM \mathcal{M}_s is finetuned using the same training data and the conventional autoregressive (AR) loss as those for \mathcal{M}_b . Notably, only the lightweight twig block is updated during the TwigVLM training, consuming only about 10% of the training time compared to its base VLM.

²For notational simplicity, we omit the visual encoder and the prediction head in the definition of \mathcal{M}_b and \mathcal{M}_s .

3.2. Efficient inference with TwigVLM

The obtained TwigVLM can be seen as a composition of a deep VLM \mathcal{M}_b and a shallow VLM \mathcal{M}_s , where their first K layers are shared with each other. We can leverage this ingenious architecture to accelerate both the prefilling and decoding stages during inference.

Prefilling acceleration via token pruning. The prefilling stage can be accelerated by applying the visual token pruning strategy. Previous methods rely on attention maps from early layers to select key visual tokens and then prune the rest. As discussed in §2.2, we have verified that the attention map of a late layer, which is closer to the prediction head, can provide more precise signals than that of an early layer. Inspired by this observation, we introduce a twig-guided token pruning (TTP) strategy which utilizes the attention map from the last twig layer to select key tokens.

As shown in Figure 4b, given the input tokens \mathbf{X} , the TTP strategy first feeds them through the first K layers of \mathcal{M}_b to obtain the latent representations $\mathbf{X}_{\mathcal{M}_b}^{(K)}$, and then feeds them through the twig block to obtain the attention map of the last twig layer $\mathbf{A}_{\mathcal{M}_s}^{(K+T)}$. After that, we use the token pruning function in Eq.(3) to obtain the representations of the retained visual tokens $\hat{\mathbf{X}}_{\mathcal{M}_b}^{(K)}$ as follows:

$$\hat{\mathbf{X}}_{\mathcal{M}_b}^{(K)} = \mathcal{P}(\mathbf{X}_{\mathcal{M}_b}^{(K)}, \mathbf{A}_{\mathcal{M}_s}^{(K+T)}, R), \quad (5)$$

where this condensed token sequence $\hat{\mathbf{X}}_{\mathcal{M}_b}^{(K)}$ is further fed through the remaining layers of \mathcal{M}_b .

To achieve aggressive token pruning with small \bar{R} , both K and R need to be small values according to Eq.(4), leading to considerable performance drops. To mitigate this issue, several works adopt *progressive* token pruning strategies [50, 62] to retain more tokens at middle layers. In addition, previous studies have shown that the visual tokens in late layers (*e.g.*, after the 20th layer) barely contribute to the prediction [64, 65]. Motivated by these works, we additionally introduce a simple *FinalWipe* strategy by removing *all* the visual tokens after the K_f -th layer (a late layer) in \mathcal{M}_b . By doing so, Eq.(4) can be reformulated as follows:

$$\bar{R} = [M \times K + R \times (K_f - K)]/L. \quad (6)$$

When \bar{R} and K are fixed, this strategy enables a larger R , which facilitates the performance of our TwigVLM.

Decoding acceleration via self-speculation. The acceleration for the decoding stage remains underexplored, especially for the long response scenarios. TwigVLM’s architecture, which contains two sub-networks, namely the deep one \mathcal{M}_b and shallow one \mathcal{M}_s , enables the self-speculative decoding (SSD) strategy [12, 28] to address this challenge. As illustrated in Figure 4c, we take the shallow model \mathcal{M}_s as a *draft* model to efficiently generate multiple subsequent tokens (*i.e.*, draft tokens), and then take the deep model \mathcal{M}_b as a *target* model to verify these tokens in parallel.

Specifically, SSD operates through multiple draft-then-verify iterations to generate the response. In each iteration, the draft model generates multiple tokens in an autoregressive manner. These tokens are then verified by feeding them through the target model in a single forward pass to determine their acceptance. Although the total computational costs are not reduced, the SSD strategy accelerates the decoding stage by processing multiple draft tokens in parallel, which maximally utilizes GPUs’ parallel computing capabilities. Moreover, the draft and target models in TwigVLM share the computation and KV-cache of the first K layers, thus achieving further efficiency gains.

It is worth noting that the SSD strategy produces exactly the same response as the target model, which means the accuracy of TwigVLM is only affected by the TTP strategy.

4. Experiments

We evaluate the performance of TwigVLM on three popular VLMs, namely LLaVA-1.5-7B [30], LLaVA-NeXT-7B [31] and Video-LLaVA-7B [26], to compare with the state-of-the-art VLM acceleration methods. After that, we conduct comprehensive ablation studies to analyze the effectiveness of the key elements of TwigVLM.

4.1. Implementation Details

Unless otherwise noted, we implement TwigVLM with the following hyper-parameters: the number of twig layers $T=3$, the token pruning position $K=2$, and the FinalWipe position $K_f=24$. Based on the default setting above, we adjust R using Eq.(6) to fairly compare TwigVLM with other methods at the same pruning ratio $1 - \bar{R}/M$. All experiments are conducted on a server with $8 \times A100$ GPUs. More implementation details are provided in the supplementary.

4.2. Evaluation Metrics

To evaluate the performance of TwigVLM, we consider two key aspects: *accuracy preservation* and *inference speedup*, which are respectively measured by the two metrics as follows. **Relative Accuracy (RelAcc)** is a widely used metric in previous works [8, 52], which calculates the proportion of the accuracy of the pruned model to the base model. When multiple benchmarks are provided, their relative accuracies are separately calculated and then averaged as the final RelAcc. **Relative Speed (RelSpd)** quantifies the relative generation speed of a pruned model compared to its base model. The generation speed is computed by dividing the number of generated tokens by the generation time—which encompasses both the prefilling and decoding stages—and then averaged across samples from a specified benchmark.

4.3. Main Results

Results on LLaVA-1.5 and LLaVA-NeXT. As shown in Tables 1 and 2, we take LLaVA-1.5-7B and LLaVA-NeXT-7B as the base VLMs and compare TwigVLM

Method	GQA	MMB	MME	VQA ^T	SQA ^I	VQA ^{V2}	RelAcc
<i>Upper Bound, 576 Tokens (100%)</i>							
LLaVA-1.5-7B	61.9	64.7	1862	58.2	69.5	78.5	100%
<i>Retain Averaged 192 Tokens (↓ 66.7%)</i>							
FastV [8]	56.5	63.7	1786	57.3	69.5	74.6	96.5%
SparseVLM [62]	57.6	62.5	1721	56.1	69.1	75.6	95.7%
PDrop [50]	57.3	63.3	1797	56.5	69.2	75.1	96.5%
MustDrop [32]	58.2	62.3	1787	56.5	69.2	76.0	96.6%
VisionZip [52]	59.3	63.0	1783	57.3	68.9	76.8	97.4%
VisionZip‡ [52]	60.1	63.4	1834	57.8	68.2	77.4	98.3%
TwigVLM (ours)	61.2	64.0	1848	58.0	68.8	78.1	99.2%
<i>Retain Averaged 128 Tokens (↓ 77.8%)</i>							
FastV	53.0	61.4	1646	56.0	69.5	69.2	92.2%
SparseVLM	56.0	60.0	1696	54.9	67.1	73.8	93.2%
PDrop	57.1	61.6	1761	56.6	68.4	72.9	95.1%
MustDrop	56.9	61.1	1745	56.3	68.5	74.6	95.1%
VisionZip	57.6	62.0	1762	56.8	68.9	75.6	96.1%
VisionZip‡	58.9	62.6	1823	57.0	68.3	76.6	97.3%
TwigVLM (ours)	60.6	63.5	1818	57.8	69.5	77.9	98.7%
<i>Retain Averaged 64 Tokens (↓ 88.9%)</i>							
FastV	44.1	45.9	1218	50.7	70.0	52.0	77.0%
SparseVLM	52.7	56.2	1505	51.8	62.2	68.2	89.9%
PDrop	47.5	58.8	1561	50.6	69.0	69.2	87.6%
FasterVLM [61]	51.5	58.5	1573	53.1	69.6	66.8	89.1%
MustDrop	53.1	60.0	1612	54.2	63.4	69.3	89.6%
VisionZip	55.1	60.1	1690	55.5	69.0	72.4	93.3%
VisionZip‡	57.0	61.5	1756	56.0	68.8	74.2	95.2%
TwigVLM (ours)	58.8	60.4	1760	55.8	70.0	75.6	96.0%

Table 1. Performance comparisons with three pruning ratios on six VLM benchmarks [13, 15, 19, 33, 34, 42]. All methods are applied on the same base model LLaVA-1.5-7B. The best result for each benchmark and pruning ratio is bolded.

with the state-of-the-art VLM acceleration methods on six commonly-used VLM benchmarks. We can see that TwigVLM consistently and significantly outperforms all its counterparts under different pruning ratios. Notably, TwigVLM achieves near-perfect performance preservation (more than 99.0%) when pruning 66.7% visual tokens on LLaVA-1.5-7B and 77.8% tokens on LLaVA-NeXT-7B, showing the superiority of our TTP strategy over existing pruning strategies. Comparisons on more benchmarks and base VLMs are provided in the supplementary.

To better understand the effectiveness of our approach, we compare TwigVLM with two representative methods [8, 52] by visualizing the attention map used for token selection. The examples in Figure 5 suggest that TwigVLM can better understand the *fine-grained* semantics in both the prompt and image, thus identifying more informative visual tokens for token pruning.

Results on Video-LLaVA for video understanding. Our TwigVLM is general and can be extended to the challenging

Method	GQA	MMB	MME	VQA ^T	SQA ^I	VQA ^{V2}	RelAcc
<i>Upper Bound, 2880 Tokens (100%)</i>							
LLaVA-NeXT-7B	64.2	67.9	1851	61.3	70.2	81.8	100%
<i>Retain Averaged 640 Tokens (↓ 77.8%)</i>							
FastV	62	65.8	1807	60	69.1	79.5	97.6%
SparseVLM	60.3	65.7	1772	57.8	67.7	77.1	95.4%
VisionZip	61.3	66.3	1787	60.2	68.1	79.1	97.1%
VisionZip‡	62.4	65.9	1778	60.8	67.9	79.9	97.4%
TwigVLM (ours)	63.4	67.4	1864	58.6	69.9	81.2	99.0%
<i>Retain Averaged 320 Tokens (↓ 88.9%)</i>							
FastV	54.9	60	1539	54.8	68.2	69.6	88.2%
SparseVLM	57.7	64.3	1694	55.9	67.3	73.4	92.3%
MustDrop	57.3	62.8	1641	59.9	68.0	73.7	92.6%
VisionZip	59.3	63.1	1702	58.9	67.3	76.2	93.8%
VisionZip‡	61.0	64.4	1770	59.3	67.5	78.4	95.8%
TwigVLM (ours)	62.2	65.0	1758	57.4	68.7	79.7	96.2%

Table 2. Performance comparisons on LLaVA-NeXT-7B. This table follows the same layout and notes as Table 1.

Method	TGIF	MSVD	MSRVTT	ActivityNet	RelAcc
Video-LLaVA-7B	47.1	69.8	56.7	43.1	100.0%
FastV	23.1	38.0	19.3	30.6	52.1%
SparseVLM	44.7	68.2	31.0	42.6	86.5%
VisionZip	42.4	63.5	52.1	43.0	93.2%
TwigVLM (ours)	44.7	68.3	54.6	41.5	96.3%

Table 3. Performance comparisons on four widely used VideoQA benchmarks [20, 51, 58]. The base model is Video-LLaVA-7B, which originally has 2,048 visual tokens. We follow the compared methods to retain 135 visual tokens.

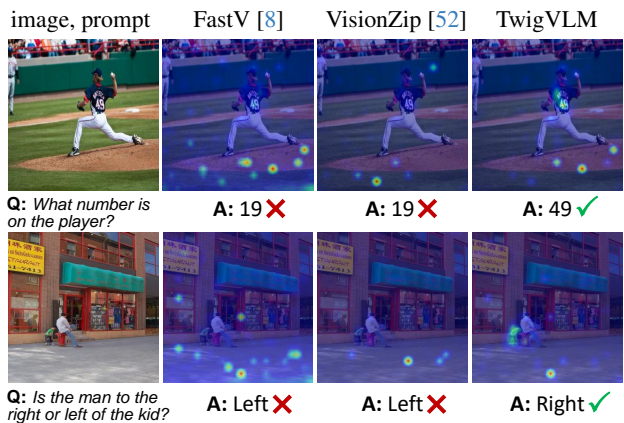


Figure 5. **Visualized attention map comparisons** of TwigVLM and two typical token pruning methods. The visualized attention maps show that TwigVLM identifies accurate visual tokens to the prompt and predicts the right answer, while both counterparts fail to do that. More examples are provided in the supplementary.

video domain seamlessly. As shown in Table 3, TwigVLM consistently surpasses all the state-of-the-art counterparts on most VideoQA benchmarks and achieves 3.1% improvements over VisionZip in terms of RelAcc. These results further validate the generalization ability of our TwigVLM.

attention source, depth D	RelAcc (%)	acceleration strategy	RelSpd (%)	initialization strategy	RelAcc (%)	RelSpd (%)
(a) VLM backbone, K	82.3	(a) token pruning (FastV [8])	104.3	(a) random init.	87.2	120.4
(b) VLM backbone, $K+T$	86.2	(b) SSD	146.7	(b) VLM layers[$L-T:L$]	90.4	131.4
(c) twig layer, $K+T$	96.0	(c) TTP & SSD	153.6	(c) VLM layers[$K:K+T$]	96.0	153.6

(a) **Visual token selection.** The attention map from the last twig layer results in the highest accuracy as it is close to the prediction head.

(b) **Acceleration strategies.** The TTP and SSD strategies are complementary and their synergy achieves the highest speedup.

(c) **Twig block initialization.** The twig layers initialized from the K -th to $(K+T)$ -th layers in base VLM achieves the best accuracy and speed.

T	RelAcc (%)	RelSpd (%)
1	93.9	154.1
2	95.2	152.6
3	96.0	153.6
4	95.8	145.4

(d) **Number of twig layers.** $T=3$ results in the highest accuracy with negligible speed degradation compared to $T=1$.

K	R	RelAcc (%)	RelSpd (%)
0	85	93.6	137.5
1	64	95.5	136.5
2	41	96.0	153.6
3	15	85.5	145.2

(e) **Pruning position.** When \bar{R} is fixed to 64, $K=2$ achieves the optimal balance between accuracy and speed.

FinalWipe	K_f	R	RelAcc (%)	RelSpd (%)
×	32	30	93.1	154.6
✓	20	50	95.8	151.3
✓	24	41	96.0	153.6
✓	28	37	95.1	154.1

(f) **FinalWipe.** The FinalWipe strategy facilitates model accuracy and $K_f=24$ is the optimal choice to balance accuracy and speed.

Table 4. **Ablation experiments for TwigVLM.** Taking LLaVA-1.5-7B as the base VLM, the relative accuracy (RelAcc) is evaluated on the six benchmarks mentioned in Table 1 and the relative speed (RelSpd) is evaluated on MM-Vet. In each table, the best result is bolded and the result with the default setting ($T=3$, $K=2$, $K_f=24$, $\bar{R}=64$) is marked in green.

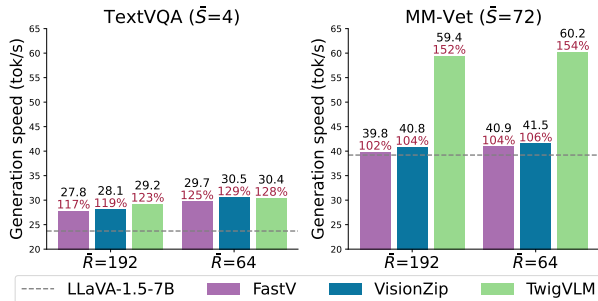


Figure 6. **Generation speed comparisons** on two benchmarks: (a) TextVQA with short responses and (b) MM-Vet with long responses. \bar{S} denotes the average number of generated tokens on the whole benchmark. The *RelSpd* of each bar is highlighted in red.

Generation speed comparisons. As mentioned above, TwigVLM can effectively accelerate the generation. To validate this, we conduct intensive experiments on two typical benchmarks TextVQA [42] and MM-Vet [57] to compare the speedup of different VLM acceleration methods based on LLaVA-1.5-7B. The results in Figure 6 show that: (i) TwigVLM achieves superior or competitive speedup in all configurations, suggesting dual advantages in speed and accuracy. (ii) All the methods attain the similar RelSpd (120%~130%) on TextVQA with short responses. In contrast, TwigVLM delivers significantly higher speedup (~150%) than FastV (~104%) and VisionZip (~106%) on MM-Vet with long responses. This reveals the superiority of our SSD strategy in long response generation. (iii) A higher pruning ratio (*i.e.*, a smaller \bar{R}) leads to more speedup on TextVQA, but has little effect on MM-Vet, which has been observed and explained in §2.3.

4.4. Ablation Studies

To validate the effectiveness of TwigVLM’s key components, we conduct ablation experiments using the default

setting ($T=3$, $K=2$, $K_f=24$, $\bar{R}=64$). Taking LLaVA-1.5-7B as the reference model, the relative accuracy (RelAcc) is evaluated on the six benchmarks mentioned in Table 1 and the relative speed (RelSpd) is evaluated on MM-Vet. Results in Table 4 are discussed in detail below.

Visual token selection. The performance of visual token pruning relies on the chosen attention map for token selection. Table 4a compares three TwigVLM variants with token pruning guided by different attention sources: (a) the K -th layer of the VLM backbone, (b) the $(K+T)$ -th layer of the VLM backbone, and (c) the last twig layer which has the same depth as (b). From the results, we can see that using the attention map of the K -th backbone layer yields the lowest accuracy (82.3%), which verifies the conclusion in §2.3 that the semantic in early-layer attention is ambiguous. With the same attention depth $D=(K+T)$, selecting tokens by the attention from the backbone (86.2%) is inferior to that from the twig layer (96.0%), indicating that the quality of the attention map is also impacted by the “distance” between the layer it is on and the prediction head.

Acceleration strategies. The inference acceleration of TwigVLM is achieved by the synergy between the twig-guided token pruning (TTP) and self-speculative decoding (SSD) strategies during prefilling and decoding, respectively. In Table 4b, we compare the three acceleration strategies as follows: (a) visual token pruning by FastV [8], (b) SSD only without token pruning, and (c) the standard TwigVLM with SSD and TTP. While FastV achieves modest speedup (104.3%), SSD delivers a remarkable improvement (146.7%) as the decoding time is longer than prefilling. Finally, the TTP and SSD strategies are complementary and their synergy achieves the highest speedup (153.6%).

Twig block initialization. The initialization strategy for twig layers has a prominent impact on TwigVLM’s performance. From Table 4c, we can see that: random initializa-

tion in (a) performs poorly due to the lack of knowledge inherited from the base VLM. Moreover, the strategy in (b) that uses the last T VLM layers to initialize the twig layers results in distinct improvements. Finally, initializing from layers K to $K+T$ achieves the best results in both accuracy and speed. The speed improvements are contributed by the higher token acceptance rate³. More detailed analyses about token acceptance rate are provided in the supplementary.

Number of twig layers. Table 4d varies the number of twig layers T from 1 to 4 to investigate its effect on TwigVLM. We observe that a single twig layer ($T=1$) leads to the highest speed but the lowest accuracy. Increasing T to 2 or 3 improves accuracy with negligible speed degradation. However, further increasing T to 4 leads to a distinct performance drop in terms of both accuracy and speed. This suggests that $T=3$ achieves an optimal balance in providing more accurate attention signals for pruning (via more twig layers) while still maintaining computational efficiency due to the high token acceptance ratio in SSD.

Pruning position. To achieve an optimal number of retained tokens when \bar{R} is fixed to 64, we use Eq.(6) to explore different combinations of K and R . Increasing K leads to a smaller R , which means a trade-off between the number of visual tokens in early layers and the number of visual tokens in subsequent layers. As shown in Table 4e, both the accuracy and speed achieve the best results at $K=2$, which is chosen in our default setting.

FinalWipe. The FinalWipe works by removing all visual tokens after the K_f -th layer. Table 4f ablates different TwigVLM variants without/with this strategy. When FinalWipe is not introduced, the accuracy is relatively low due to the insufficiency of retained tokens. Introducing FinalWipe facilitates accuracy with limited speed drop, which can be explained by the fact that the visual tokens become less important in late layers. $K_f=24$ achieves a good balance between accuracy and speed, thus is used as default.

5. Related Work

Inference acceleration for LLMs. Accelerating the inference process of LLMs has attracted significant attention from both academia and industry. Although various efficient model architectures have been proposed successively [16, 27, 43], they often need to be trained from scratch, thus incurring substantial costs. Consequently, the research of accelerating off-the-shelf LLMs has been extensively investigated from the prefilling and decoding stages of inference, respectively. In the prefilling stage, acceleration is achieved by redundant token reduction [21, 38] and attention operator optimization [10, 11]. In the decoding stage, techniques such as dynamic reduction of KV-cache [49, 63] and specu-

lative decoding [5, 12, 23, 28] are introduced. In particular, speculative decoding performs parallel verification of draft tokens to boost GPU utilization, thus significantly improving the speed.

Visual token reduction for VLMs. Unlike acceleration techniques for LLMs, token reduction methods for VLMs mainly address the problem of visual token redundancy to improve inference efficiency [65]. The pioneering work of FastV [8] first studies this redundancy phenomenon, revealing that pruning visual tokens at an early layer of the VLM can achieve acceleration while preserving the majority of the model’s accuracy. Following this paradigm, subsequent studies have introduced adaptive or hierarchical pruning strategies [18, 32, 48, 55, 56, 62] and training-based adoption [7, 50, 64] to further reduce the accuracy drop. Meanwhile, there is another line of studies that performs more aggressive token reduction by pruning or merging visual tokens in the visual encoding stage [2, 41, 45, 52, 61]. However, the accuracy of these pruned models is suboptimal as they are unaware of the textual prompt when pruning visual tokens. Finally, although the above methods effectively accelerate the prefilling stage of VLMs, their speedup in the decoding stage is limited.

Collaborative decoding of small-large VLMs. Beyond visual token reduction, some recent works have explored another way, *i.e.*, the collaborative decoding of small and large VLMs, for VLM acceleration [14, 66]. Specifically, Gagrani *et al.* introduce a multimodal speculative decoding method, where a small language-only LLM is adopted to efficiently generate draft tokens and followed by the verification by a large VLM [14]. Similarly, Zhao *et al.* use an small VLM for early-exit prediction, invoking the large VLM only when the prediction confidence is low [66]. However, both methods above require an pre-existing and high-capable small model with the same vocabulary as the large model, which severely restricts the choice of VLMs.

6. Conclusion

We present TwigVLM, a conceptually simple yet effective approach for VLM acceleration. Unlike existing purely token pruning methods, TwigVLM trains a lightweight twig block upon an early layer of the base VLM. After that, the learned twig block is used in both the prefilling and decoding stages to obtain better accuracy retention and faster generation speed simultaneously. Extensive ablation, comparative experiments, and comprehensive analyses on a wide range of VLM benchmarks show the superiority of TwigVLM over previous state-of-the-art methods. We hope our work may serve as a solid baseline to inspire future research on VLM acceleration.

³The token acceptance rate measures how often verification accepts each of the draft tokens [12].

A. More Implementation Details

TwigVLM training. As described in the main text, the twig block is trained by finetuning the shallow VLM \mathcal{M}_s . Specifically, \mathcal{M}_s is initialized with the weights of the first $K+T$ layers and the prediction head of the corresponding base VLM \mathcal{M}_b . During finetuning, only the last T layers and the prediction head—collectively termed the twig block—are updated, while the first K layers remain frozen. This process follows the same training manner to train the base VLM \mathcal{M}_b . Theoretically, any suitable multimodal instruction tuning dataset can be employed to finetune \mathcal{M}_s .

In our experiments, we utilize the LLaVA-665K dataset [30] to train the twig blocks for the LLaVA-1.5-7B and LLaVA-NeXT-7B models, and combine the LLaVA-665K and VideoInstruct-100K datasets [26, 37] for the Video-LLaVA-7B model. The optimization hyper-parameters are detailed in Table 5. All training is performed on a server equipped with 8 NVIDIA A100 GPUs. Under these conditions, the training process is highly efficient, requiring only approximately 10% of the time needed to train the corresponding base VLM, *e.g.*, training the twig block for the LLaVA-1.5-7B model takes about 1 hour, while the training of the original LLaVA-1.5-7B takes about 12 hours.

config	setting
optimizer	AdamW
weight decay	0.
optimizer momentum	$\beta_1, \beta_2=0.9, 0.98$
batch size	128
learning rate schedule	cosine decay
peak learning rate	5e-5
warm-up strategy	linearly warm-up
warm-up ratio	0.03
training epochs	1

Table 5. **Training settings.** These hyper-parameters are shared across all the TwigVLM models in our experiments.

Twig-guided token pruning (TTP). During inference, TwigVLM leverages the TTP strategy to perform token pruning over the base VLM: (i) at the K -th layer, selecting R key visual tokens (output by the K -th layer) and discarding the rest tokens guided by the attention map from the last twig layer, and (ii) applying the FinalWipe strategy to further remove all the visual tokens after the K_f -th layer. Therefore, we adjust the value of R to satisfy different pruning ratios calculated by the average number of retained visual tokens \bar{R} . Table 6 shows the default pruning settings for TwigVLM under different pruning ratios.

\bar{R}	pruning ratio	K	R	K_f
192	66.7%	2	227	24
128	77.8%	2	134	24
64	88.9%	2	41	24

Table 6. **Pruning settings.** These hyper-parameters correspond to the default TTP settings of different pruning ratios.

Algorithm 1 Pseudocode of TwigVLM’s inference process

```

# bVLM: the base VLM model, i.e., M_b
# twig: the twig block
# K: Number of shared low layers
# K_f: The position to apply FinalWipe
# R: Number of retained visual tokens when pruning
# delta: Maximum draft token length
# theta: Confidence threshold to stop draft

def sVLM_forward(tokens):
    X_k = bVLM.forward_low_layers(tokens, k=K)
    prob, Attn_last = twig.forward(X_k)
    a_i = argmax(prob)
    return X_k, prob, Attn_last, a_i

def TwigVLM_inference(img, ques):
    draft_toks = [] # temporary buffer for draft tokens
    final_resp = [] # buffer for final response

    # Prefilling stage of sVLM
    X_k, _, Attn, a_i = sVLM_forward((img, ques))
    draft_toks.append(a_i)

    # Prune visual tokens in X_k using Eq. (5)
    # X_k_b means shared token latents for bVLM
    X_k_b = pruning(X_k, Attn, r=R)

    # The loop of self speculative decoding
    while EOS_TOKEN not in final_resp:
        X_k, prob, _, a_i = sVLM_forward(a_i)
        draft_toks.append(a_i)
        X_k_b = concat(X_k_b, X_k, axis=1)

    # the condition to stop draft and verify
    if len(draft_toks) >= delta or prob < theta:
        # removing all visual tokens after layer K_f
        tgt_probs = bVLM.forward_high_layers(
            X_k_b, k=K, fianl_wipe=K_f)
        # verification
        right_toks = [a for a, p in zip(draft_toks, tgt_probs)
            if argmax(p) == a]
        right_toks.append(argmax(tgt_probs[-1]))
        final_resp.extend(right_toks)
        # reset temporary variables
        draft_toks = []
        X_k_b = None
        a_i = final_resp[-1]

    return final_resp

```

Self-speculative decoding (SSD). For efficient generation of long responses, TwigVLM applies the SSD strategy by using the \mathcal{M}_s as the *draft* model and \mathcal{M}_b as the *target* model. Specifically, in each SSD iteration, the draft model efficiently predicts $\delta = 5$ subsequent draft tokens in an autoregressive manner. To further improve efficiency, this draft generation process is equipped with an early-exit mechanism that allows the draft model to stop generation if the probability of the current predicted token falls below a predefined threshold $\theta = 0.6$. The target model then verifies these generated draft tokens in parallel, accepts those matching the target model’s predictions, and then predicts a next token by itself. The iteration repeats until the <EOS> token is generated. Note that the TTP and SSD strategies can be seamlessly integrated, as detailed in Algorithm 1.

B. More Experimental Results

Token acceptance rate in SSD. In the context of speculative decoding methods [12, 23, 28], the token acceptance

ablation variant	TokAR (%)	RelSpd (%)
<i>Twig block initialization</i> (Table 4c in main text)		
(a) random init.	37.7	120.4
(b) VLM layers[$L:T:L$]	44.1	131.4
(c) VLM layers[$K:K+T$]	57.4	153.6
<i>Number of twig layers</i> (Table 4d in main text)		
(d) $T = 1$	48.7	154.1
(e) $T = 2$	53.4	152.6
(f) $T = 3$	57.4	153.6
(g) $T = 4$	58.1	145.4

Table 7. **Token acceptance rate in SSD.** We evaluate the token acceptance rate (TokAR) of the variants in the ablation experiments of the main text.

rate (*abbr.* TokAR) serves as a critical metric for assessing the efficacy of these approaches. TokAR is defined as the proportion of the draft tokens generated by the draft model that are subsequently accepted by the target model. In TwigVLM, TokAR plays a key role, which is influenced by the effectiveness of the twig block and has a significant impact on model’s generation speed.

To analyze how TokAR is influenced by the design choices in TwigVLM, we evaluate this metric on several representative variants from the ablation studies presented in the main text. From the results shown in Table 7, we have the following findings: (i) A more effective draft model can be trained by only modifying the initialization strategy without altering the architecture. The variant (c) achieves the highest TokAR (57.4%) and thus the highest generation speedup. (ii) Increasing the number of twig layers T introduces more computational costs while improving TokAR at the same time. As a result, the RelSpd exhibits only a modest decline when T increases from 1 to 3. However, it drops distinctly at $T=4$, which indicates that TokAR begins to saturate. These findings suggest that TwigVLM achieves higher speedup by striking an optimal balance between TokAR and computation costs of the draft model.

More accuracy comparisons on benchmarks. To further demonstrate the superiority of TwigVLM, we present additional experimental results on a larger base VLM and more benchmarks, respectively.

Table 8 provides the accuracy comparisons on a larger LLaVA-1.5-13B model. TwigVLM consistently achieves the best overall RelAcc compared to all the counterparts, with its superiority being more significant as the increase of pruning ratios. These results verify the scalability and generalization ability of TwigVLM in accelerating large VLMs.

Taking LLaVA-1.5-7B as the base VLM, Table 9 compares the accuracies between TwigVLM and other visual token pruning methods on *nine* VLM benchmarks under

Method	GQA	MMB	MME	VQA ^T	SQA ^I	VQA ^{V2}	RelAcc
<i>Upper Bound, 576 Tokens (100%)</i>							
LLaVA-1.5-13B	63.2	67.7	1818	61.3	72.8	80.0	100%
<i>Retain Averaged 192 Tokens (↓ 66.7%)</i>							
FastV	60.3	67.4	1807	60.4	74.0	77.7	98.6%
VisionZip	59.1	66.9	1754	59.5	73.5	78.1	97.4%
VisionZip‡	61.6	67.1	1790	59.9	72.7	78.6	98.5%
TwigVLM (ours)	62.5	68.6	1840	60.4	73.1	79.4	99.9%
<i>Retain Averaged 128 Tokens (↓ 77.8%)</i>							
FastV	57.5	65.9	1758	58	73.8	74.3	95.7%
VisionZip	57.9	66.7	1743	58.7	74.0	76.8	96.6%
VisionZip‡	60.1	67.6	1736	59.2	73.0	77.6	97.4%
TwigVLM (ours)	61.2	66.9	1811	60.2	73.4	79.1	98.9%
<i>Retain Averaged 64 Tokens (↓ 88.9%)</i>							
FastV	50.1	55.9	1408	52.2	73.2	61.1	83.6%
VisionZip	56.2	64.9	1676	57.4	74.4	73.7	94.2%
VisionZip‡	58.1	65.6	1671	58.5	72.3	75.2	94.9%
TwigVLM (ours)	60.0	67.4	1765	58.4	72.4	77.0	97.1%

Table 8. Performance comparisons of TwigVLM with other token pruning methods on **LLaVA-1.5-13B**.

three different pruning ratios. TwigVLM consistently outperforms or matches its counterparts on all benchmarks and pruning ratios, achieving the best overall RelAcc. In particular, TwigVLM even surpasses the upper bound given by the base VLM in RelAcc (100.6%) with a 66.7% pruning ratio, demonstrating its spectacular effectiveness and robustness in accelerating VLMs to deal with various tasks.

C. More Visualized Results

In this section, we provide more visualized results to validate the effectiveness of TwigVLM’s two key components: the twig-guided visual token pruning (TTP) and self-speculative decoding (SSD). We use LLaVA-1.5-7B as the base VLM in the following experiments.

Visual token pruning. To better understand the effectiveness of the proposed TTP strategy, we compare TwigVLM with two representative token pruning methods, namely FastV [8] and VisionZip [52], by visualizing their attention map for token selection and providing the corresponding answer predictions. We provide 16 examples from the GQA and TextVQA benchmarks. As illustrated in Figure 7, TwigVLM demonstrates superior ability to comprehend the semantics in both the textual prompt and image, and accurately identify task-specific image patches (*i.e.*, visual tokens), thereby activating more informative visual tokens for token pruning. In contrast, FastV and VisionZip often fail to capture the fine-grained visual details, leading to suboptimal token selection and incorrect predictions. Notably, even though TwigVLM predicts an incorrect answer, its activated visual tokens according to the attention map is reasonable.

Method	GQA	MMB	MME	VQA ^T	SQA ^I	VQA ^{V2}	POPE	MMMU	MM-Vet	RelAcc
<i>Upper Bound, 576 Tokens (100%)</i>										
LLaVA-1.5-7B	61.9	64.7	1862	58.2	69.5	78.5	85.9	36.3	31.1	100%
<i>Retain Averaged 192 Tokens (↓ 66.7%)</i>										
FastV [8]	56.5	63.7	1786	57.3	69.5	74.6	79.2	35.7	28.1	95.6%
SparseVLM [62]	57.6	62.5	1721	56.1	69.1	75.6	83.6	33.8	31.5	96.2%
PDrop [50]	57.3	63.3	1797	56.5	69.2	75.1	82.3	-	-	96.4%
MustDrop [32]	58.2	62.3	1787	56.5	69.2	76.0	82.6	-	-	96.6%
VisionZip [52]	59.3	63.0	1783	57.3	68.9	76.8	85.3	36.6	31.7	98.5%
VisionZip‡ [52]	60.1	63.4	1834	57.8	68.2	77.4	84.9	36.2	32.6	99.2%
TwigVLM (ours)	61.2	64.0	1848	58.0	68.8	78.1	87.2	36.6	34.1	100.8%
<i>Retain Averaged 128 Tokens (↓ 77.8%)</i>										
FastV	53.0	61.4	1646	56.0	69.5	69.2	73.2	36.3	28.0	92.1%
SparseVLM	56.0	60.0	1696	54.9	67.1	73.8	80.5	33.8	30.0	93.6%
PDrop	57.1	61.6	1761	56.6	68.4	72.9	82.3	-	-	95.2%
MustDrop	56.9	61.1	1745	56.3	68.5	74.6	78.7	-	-	94.6%
VisionZip	57.6	62.0	1762	56.8	68.9	75.6	83.2	37.9	32.6	98.1%
VisionZip‡	58.9	62.6	1823	57.0	68.3	76.6	83.7	37.3	32.9	98.8%
TwigVLM (ours)	60.6	63.5	1818	57.8	69.5	77.9	86.6	36.6	32.8	99.9%
<i>Retain Averaged 64 Tokens (↓ 88.9%)</i>										
FastV	44.1	45.9	1218	50.7	70.0	52.0	55.6	34.0	17.8	75.3%
SparseVLM	52.7	56.2	1505	51.8	62.2	68.2	75.1	32.7	23.3	85.6%
PDrop	47.5	58.8	1561	50.6	69.0	69.2	55.9	-	-	84.4%
FasterVLM [61]	51.5	58.5	1573	53.1	69.6	66.8	67.2	-	27.5	87.6%
MustDrop	53.1	60.0	1612	54.2	63.4	69.3	68.0	-	-	88.1%
VisionZip	55.1	60.1	1690	55.5	69.0	72.4	77.0	36.2	31.7	94.5%
VisionZip‡	57.0	61.5	1756	56.0	68.8	74.2	80.9	35.6	30.2	95.6%
TwigVLM (ours)	58.8	60.4	1760	55.8	70.0	75.6	82.7	35.9	31.1	96.8%

Table 9. Performance of TwigVLM on LLaVA-1.5-7B compared to existing methods under three different pruning ratios. The best result for each benchmark and pruning ratio is bolded.

This suggests that TwigVLM’s occasional failures may not be caused by the visual token pruning, but due to the limitations of the base VLM. These findings verify and explain the effectiveness of the TTP strategy.

Self-speculative decoding. To better understand the decoding behavior of the SSD strategy in TwigVLM, we show 8 examples of generated long responses on MM-Vet. From the results in Figure 8, we have two key observations: (i) In general, the proportion of accepted tokens (in green) surpasses that of the corrected tokens (in black) by the target model, indicating that TwigVLM achieves significant speedup through its high token acceptance rate. (ii) The majority of *easy* tokens, such as those associated with grammar and punctuation, are readily accepted. In contrast, the *hard* tokens, which often demand complex reasoning, have a high probability to be corrected by the target model. In practice, the proportion of easy tokens is usually larger than

the hard ones, which confirms the the effectiveness of our SSD strategy in accelerating the decoding stage while maintaining the generation quality.

D. Evaluation Benchmarks

In this section, we provide a brief overview of the benchmarks used in our experiments.

GQA [19] is a benchmark that focuses on visual scene understanding and reasoning, leveraging scene graphs, questions, and images. It incorporates spatial relationships and object properties, posing challenges for models to perform accurate visual reason under complex visual environments.

MMBench [33] adopts a hierarchical evaluation approach with three levels: Level-1 (perception and reasoning), Level-2 (six sub-abilities), and Level-3 (20 specific dimensions). This structured framework allows for a comprehen-

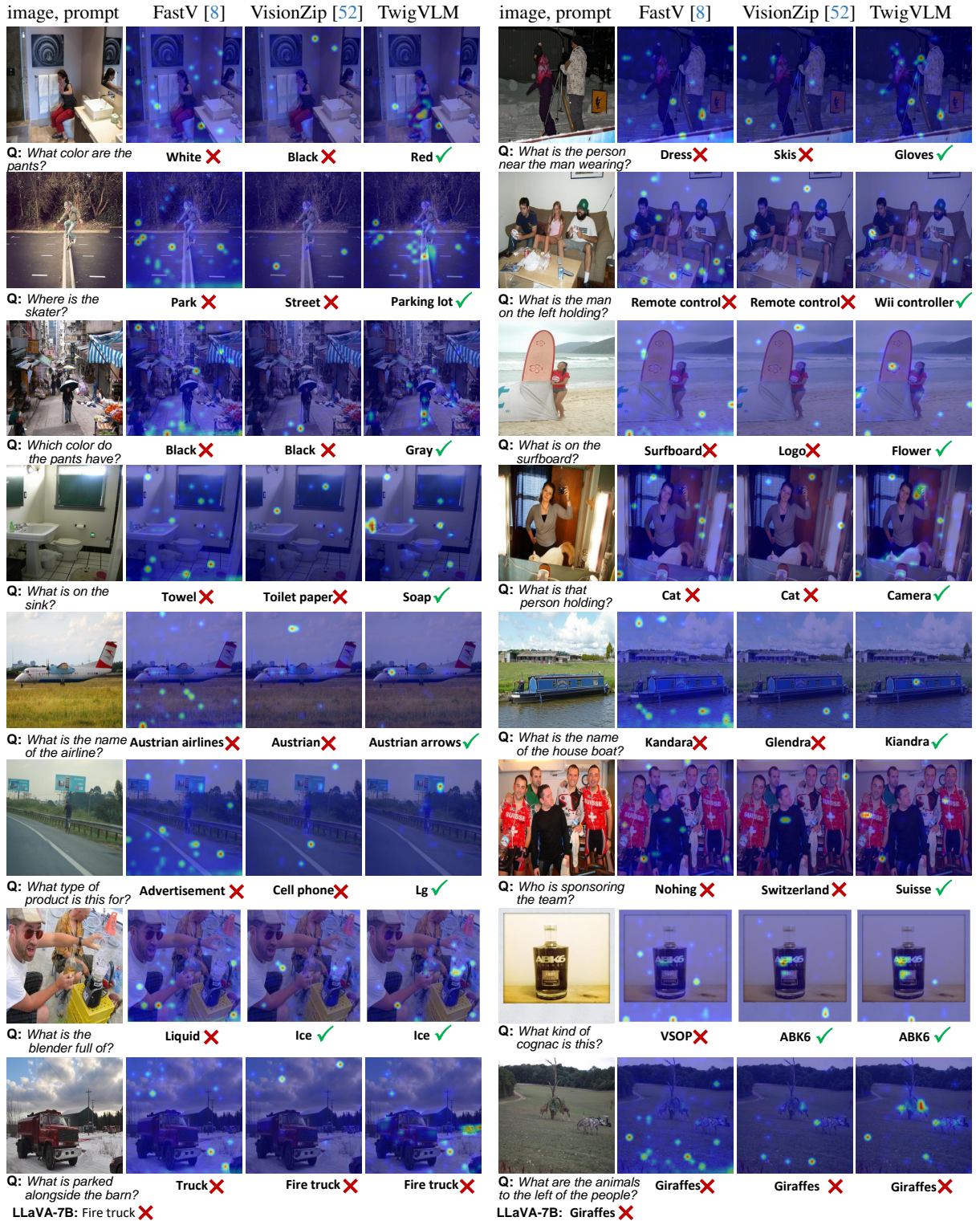


Figure 7. Visualization of attention maps and predictions for FastV [8], VisionZip [52], and our TwigVLM on the examples chosen from the GQA [19] and TextVQA [42]. For the examples in the last row, we additionally provide the predictions from the LLaVA-1.5-7B.



Q: Is that wine in the background?

A: No, there is no wine in the background. The image features a pizza and a soda in a box, along with a laptop and a potted plant.



Q: what is the green logo on the car?

A: The green logo on the car is the Monster Energy logo.



Q: Introduce the player on the right.

A: The player on the right is named Kaká, and he is wearing a jersey with the number 8.



Q: Is there any reflection of zebra in water?

A: Yes, there is a reflection of the zebra in the water.



Q: Can you give a short introduction to this painting?

A: The painting is a famous artwork by Vincent Van Gogh, featuring a night scene with a sky filled with stars. The scene is set in a village, with a church steeple visible in the distance. The painting captures the beauty of the night sky and the tranquility of the village, creating a serene atmosphere. The combination of the stars, the church steeple, and the village buildings make this painting a captivating representation of the artist's vision.



Q: Can you give a short introduction to this person?

A: The image features a statue of an old man with a long beard, sitting and holding a staff in his hands. The statue appears to be a representation of a wise or respected figure, possibly a religious leader or a historical figure. The statue is situated in front of a building, possibly a temple or a museum, and it serves as a symbol of wisdom, knowledge, or spiritual guidance.



Q: Provide a detailed description of the given image.

A: The image features a dining table with a white plate filled with a variety of breakfast foods. The plate contains eggs, toast, and a selection of fruits, including strawberries and blueberries. There are also sausages on the plate, adding to the delicious assortment of breakfast items. A cup of coffee is placed next to the plate, completing the breakfast setup. A fork is positioned on the table, ready for use. The table setting is inviting and perfect for a morning meal.



Q: Can you give a short introduction to this movie?

A: The movie "The Dark Knight" is a 2008 superhero film directed by Christopher Nolan. It is the second installment in the Batman film series and stars Heath Ledger as the Joker, along with Christian Bale as Batman/Bruce Wayne, Michael Caine as Alfred, and Maggie Gyllenhall as Rachel Dawes. The film follows Batman as he battles the Joker, a psychopathic criminal mastermind who seeks to take over Gotham City. The movie is known for its intense action sequences, complex plot, and the iconic performance of Heath Ledger as the Joker.

Figure 8. Examples of the generated responses using the self-speculative decoding (SSD) on MM-Vet [57], with accepted tokens by the target model being highlighted in green.

sive evaluation of model performance, making it an effective tool for assessing a wide range of visual understanding capabilities. We denote it as “MMB” in the main text.

MME [13] assesses models across 14 subtasks that probe both perceptual and cognitive skills. Carefully crafted instruction-answer pairs guarantee a fair and comprehen-

sive evaluation of a model’s multimodal performance. The final score reported on this benchmark is the summation of both the perception and cognition scores.

ScienceQA [34] spans multiple scientific fields, including natural, language, and social sciences, with questions organized into 26 topics, 127 categories, and 379 skills. It evaluates a model’s multimodal comprehension, multi-step reasoning, and interpretability, providing a rich testbed for assessing scientific knowledge application in visual contexts. In our experiments, we only evaluate the performance on the samples with images, denoted as “SQA^I” in the experimental tables.

VQA-v2 [15] is a large-scale benchmark featuring 265K images of real-world scenes and objects, with each image paired with open-ended questions and 10 human-provided ground truth answers.

TextVQA [42] tests a model’s ability to process and reason about text embedded within images. By requiring the integration of visual and textual information, it serves as a critical benchmark for evaluating text-based reasoning in visual contexts. To save space, we denote it as “VQA^T” in the experimental tables.

POPE [24] targets object hallucination evaluation by posing binary questions about object presence in images. It employs metrics such as Accuracy, Recall, Precision, and F1 score across three sampling methods. The reported score is calculated by the mean accuracy over the three indicators: adversarial, random, and popular.

MMMU [59] challenges models with tasks requiring college-level expertise and reasoning skills. It comprises 11.5K questions drawn from exams, quizzes, and textbooks, spanning six key disciplines: Art & Design, Business, Science, Health & Medicine, Humanities & Social Science, and Tech & Engineering. Featuring 30 subjects and 183 sub-fields, MMMU involves diverse image types, e.g., charts, diagrams, and chemical structures, demanding advanced perceptual and domain-specific reasoning abilities akin to those of human experts.

MM-Vet [57] evaluates six fundamental vision-language capabilities: recognition, OCR, knowledge, language generation, spatial awareness, and mathematical reasoning. It examines 16 specific combinations of these skills through quantitative metrics, offering a nuanced perspective on a model’s proficiency in tackling intricate multimodal tasks.

TGIF-QA [20] adapts image question answering to the video domain, specifically targeting GIFs. With 165K question-answer pairs, it introduces tasks such as counting repetitions, identifying repeating actions, detecting state transitions, and frame-specific QA. These tasks demand detailed spatio-temporal analysis, making it a rigorous test for video comprehension. We employ GPT-3.5-turbo to assist

in the evaluation of accuracy (same for the following three benchmarks). We denote it as “TGIF” in the main text.

MSVD-QA [51] is built on the Microsoft Research Video Description (MSVD) dataset [6], which includes 1,970 video clips and about 50,500 QA pairs. Its open-ended questions span five types—what, who, how, when, and where—offering a diverse and widely used evaluation for video question answering and captioning tasks. We denote it as “MSVD” in the main text.

MSRVTT-QA [6] comprises 10K video clips and 243K QA pairs, presenting a complex challenge due to the need to process both visual and temporal information. Like MSVD-QA, it features five question types, testing a model’s ability to understand and reason about dynamic video content. We denote it as “MSRVTT” in the main text.

ActivityNet-QA [58] offers 58K human-annotated question-answer pairs across 5.8K videos from the ActivityNet dataset. Its questions include motion, spatial relationships, and temporal dynamics, requiring long-term spatio-temporal reasoning and making it a popular benchmark for evaluating advanced video understanding abilities. We denote it as “ActivityNet” in the main text.

References

- [1] Jinze Bai, Shuai Bai, Shusheng Yang, Shijie Wang, Sinan Tan, Peng Wang, Junyang Lin, Chang Zhou, and Jingren Zhou. Qwen-vl: A frontier large vision-language model with versatile abilities. *arXiv preprint arXiv:2308.12966*, 2023. 1
- [2] Daniel Bolya, Cheng-Yang Fu, Xiaoliang Dai, Peizhao Zhang, Christoph Feichtenhofer, and Judy Hoffman. Token merging: Your vit but faster. In *The Eleventh International Conference on Learning Representations*, 2023. 8
- [3] Anthony Brohan, Noah Brown, Justice Carbajal, Yevgen Chebotar, Xi Chen, Krzysztof Choromanski, Tianli Ding, Danny Driess, Avinava Dubey, Chelsea Finn, et al. Rt-2: Vision-language-action models transfer web knowledge to robotic control. *arXiv preprint arXiv:2307.15818*, 2023. 1
- [4] Tom Brown, Benjamin Mann, Nick Ryder, Melanie Subbiah, Jared D Kaplan, Prafulla Dhariwal, Arvind Neelakantan, Pranav Shyam, Girish Sastry, Amanda Askell, Sandhini Agarwal, Ariel Herbert-Voss, Gretchen Krueger, Tom Henighan, Rewon Child, Aditya Ramesh, Daniel Ziegler, Jeffrey Wu, Clemens Winter, Chris Hesse, Mark Chen, Eric Sigler, Mateusz Litwin, Scott Gray, Benjamin Chess, Jack Clark, Christopher Berner, Sam McCandlish, Alec Radford, Ilya Sutskever, and Dario Amodei. Language models are few-shot learners. In *Advances in Neural Information Processing Systems*, pages 1877–1901, 2020. 1
- [5] Tianle Cai, Yuhong Li, Zhengyang Geng, Hongwu Peng, Jason D Lee, Deming Chen, and Tri Dao. Medusa: Simple llm inference acceleration framework with multiple decoding heads. *arXiv preprint arXiv:2401.10774*, 2024. 8
- [6] David L. Chen and William B. Dolan. Collecting highly parallel data for paraphrase evaluation. In *ACL*, Portland, OR, 2011. 14

- [7] Jieneng Chen, Luoxin Ye, Ju He, Zhao-Yang Wang, Daniel Khashabi, and Alan Yuille. Llavolta: Efficient multi-modal models via stage-wise visual context compression. *arXiv preprint arXiv:2406.20092*, 2024. 8
- [8] Liang Chen, Haozhe Zhao, Tianyu Liu, Shuai Bai, Junyang Lin, Chang Zhou, and Baobao Chang. An image is worth 1/2 tokens after layer 2: Plug-and-play inference acceleration for large vision-language models. In *European Conference on Computer Vision*, pages 19–35. Springer, 2024. 1, 2, 3, 5, 6, 7, 8, 10, 11, 12
- [9] Zhe Chen, Weiyun Wang, Hao Tian, Shenglong Ye, Zhangwei Gao, Erfei Cui, Wenwen Tong, Kongzhi Hu, Jiapeng Luo, Zheng Ma, et al. How far are we to gpt-4v? closing the gap to commercial multimodal models with open-source suites. *Science China Information Sciences*, 67(12):220101, 2024. 1
- [10] Steve Dai, Hasan Genc, Rangharajan Venkatesan, and Brucek Khailany. Efficient transformer inference with statically structured sparse attention. In *2023 60th ACM/IEEE Design Automation Conference (DAC)*, pages 1–6. IEEE, 2023. 8
- [11] Tri Dao, Daniel Y. Fu, Stefano Ermon, Atri Rudra, and Christopher Ré. FlashAttention: Fast and memory-efficient exact attention with IO-awareness. In *Advances in Neural Information Processing Systems (NeurIPS)*, 2022. 8
- [12] Mostafa Elhoushi, Akshat Shrivastava, Diana Liskovich, Basil Hosmer, Bram Wasti, Liangzhen Lai, Anas Mahmoud, Bilge Acun, Saurabh Agarwal, Ahmed Roman, et al. Layer-skip: Enabling early exit inference and self-speculative decoding. *arXiv preprint arXiv:2404.16710*, 2024. 1, 2, 4, 5, 8, 9
- [13] Chaoyou Fu, Peixian Chen, Yunhang Shen, Yulei Qin, Mengdan Zhang, Xu Lin, Zhenyu Qiu, Wei Lin, Jinrui Yang, Xiawu Zheng, et al. Mme: A comprehensive evaluation benchmark for multimodal large language models. *arXiv preprint arXiv:2306.13394*, 2023. 6, 13
- [14] Mukul Gagrani, Raghavv Goel, Wonseok Jeon, Junyoung Park, Mingu Lee, and Christopher Lott. On speculative decoding for multimodal large language models. In *Proceedings of the IEEE/CVF Conference on Computer Vision and Pattern Recognition*, pages 8285–8289, 2024. 8
- [15] Yash Goyal, Tejas Khot, Douglas Summers-Stay, Dhruv Batra, and Devi Parikh. Making the v in vqa matter: Elevating the role of image understanding in visual question answering. In *Proceedings of the IEEE/CVF Conference on Computer Vision and Pattern Recognition*, pages 6904–6913, 2017. 6, 14
- [16] Albert Gu and Tri Dao. Mamba: Linear-time sequence modeling with selective state spaces. In *First Conference on Language Modeling*, 2024. 8
- [17] Daya Guo, Dejian Yang, Haowei Zhang, Junxiao Song, Ruoyu Zhang, Runxin Xu, Qihao Zhu, Shirong Ma, Peiyi Wang, Xiao Bi, et al. Deepseek-r1: Incentivizing reasoning capability in llms via reinforcement learning. *arXiv preprint arXiv:2501.12948*, 2025. 1
- [18] Yuhang Han, Xuyang Liu, Pengxiang Ding, Donglin Wang, Honggang Chen, Qingsen Yan, and Siteng Huang. Rethinking token reduction in mllms: Towards a unified paradigm for training-free acceleration. *arXiv preprint arXiv:2411.17686*, 2024. 8
- [19] Drew A Hudson and Christopher D Manning. Gqa: A new dataset for real-world visual reasoning and compositional question answering. In *Proceedings of the IEEE/CVF Conference on Computer Vision and Pattern Recognition*, 2019. 3, 6, 11, 12
- [20] Yunseok Jang, Yale Song, Youngjae Yu, Youngjin Kim, and Gunhee Kim. Tgif-qa: Toward spatio-temporal reasoning in visual question answering. In *Proceedings of the IEEE conference on computer vision and pattern recognition*, pages 2758–2766, 2017. 6, 14
- [21] Huiqiang Jiang, Qianhui Wu, Chin-Yew Lin, Yuqing Yang, and Lili Qiu. Lmlingua: Compressing prompts for accelerated inference of large language models. In *Proceedings of the 2023 Conference on Empirical Methods in Natural Language Processing*, pages 13358–13376, 2023. 8
- [22] Moo Jin Kim, Karl Pertsch, Siddharth Karamcheti, Ted Xiao, Ashwin Balakrishna, Suraj Nair, Rafael Rafailov, Ethan Foster, Grace Lam, Pannag Sanketi, et al. Openvla: An open-source vision-language-action model. *arXiv preprint arXiv:2406.09246*, 2024. 1
- [23] Yaniv Leviathan, Matan Kalman, and Yossi Matias. Fast inference from transformers via speculative decoding. In *International Conference on Machine Learning*, pages 19274–19286. PMLR, 2023. 8, 9
- [24] Yifan Li, Yifan Du, Kun Zhou, Jinpeng Wang, Wayne Xin Zhao, and Ji-Rong Wen. Evaluating object hallucination in large vision-language models. *arXiv:2305.10355*, 2023. 14
- [25] Yanwei Li, Yuechen Zhang, Chengyao Wang, Zhisheng Zhong, Yixin Chen, Ruihang Chu, Shaoteng Liu, and Jiaya Jia. Mini-gemini: Mining the potential of multi-modality vision language models. *arXiv preprint arXiv:2403.18814*, 2024. 1
- [26] Bin Lin, Yang Ye, Bin Zhu, Jiayi Cui, Munan Ning, Peng Jin, and Li Yuan. Video-llava: Learning united visual representation by alignment before projection. *arXiv preprint arXiv:2311.10122*, 2023. 5, 9
- [27] Aixin Liu, Bei Feng, Bing Xue, Bingxuan Wang, Bochao Wu, Chengda Lu, Chenggang Zhao, Chengqi Deng, Chenyu Zhang, Chong Ruan, et al. Deepseek-v3 technical report. *arXiv preprint arXiv:2412.19437*, 2024. 8
- [28] Fangcheng Liu, Yehui Tang, Zhenhua Liu, Yunsheng Ni, Duyu Tang, Kai Han, and Yunhe Wang. Kangaroo: Lossless self-speculative decoding for accelerating llms via double early exiting. *Advances in Neural Information Processing Systems*, 37:11946–11965, 2025. 5, 8, 9
- [29] Haotian Liu, Chunyuan Li, Qingyang Wu, and Yong Jae Lee. Visual instruction tuning. In *Advances in Neural Information Processing Systems*, pages 34892–34916, 2023. 1
- [30] Haotian Liu, Chunyuan Li, Yuheng Li, and Yong Jae Lee. Improved baselines with visual instruction tuning. In *Proceedings of the IEEE/CVF Conference on Computer Vision and Pattern Recognition*, pages 26296–26306, 2024. 1, 3, 4, 5, 9
- [31] Haotian Liu, Chunyuan Li, Yuheng Li, Bo Li, Yuanhan Zhang, Sheng Shen, and Yong Jae Lee. Llava-next: Improved reasoning, ocr, and world knowledge, 2024. 5

- [32] Ting Liu, Liangtao Shi, Richang Hong, Yue Hu, Qianjun Yin, and Linfeng Zhang. Multi-stage vision token dropping: Towards efficient multimodal large language model. *arXiv preprint arXiv:2411.10803*, 2024. 2, 3, 6, 8, 11
- [33] Yuan Liu, Haodong Duan, Yuanhan Zhang, Bo Li, Songyang Zhang, Wangbo Zhao, Yike Yuan, Jiaqi Wang, Conghui He, Ziwei Liu, et al. Mmbench: Is your multi-modal model an all-around player? In *European Conference on Computer Vision*, pages 216–233. Springer, 2025. 6, 11
- [34] Pan Lu, Swaroop Mishra, Tanglin Xia, Liang Qiu, Kai-Wei Chang, Song-Chun Zhu, Oyvind Tafjord, Peter Clark, and Ashwin Kalyan. Learn to explain: Multimodal reasoning via thought chains for science question answering. *Advances in Neural Information Processing Systems*, 35:2507–2521, 2022. 6, 14
- [35] Chuwei Luo, Yufan Shen, Zhaoqing Zhu, Qi Zheng, Zhi Yu, and Cong Yao. Layoutllm: Layout instruction tuning with large language models for document understanding. In *Proceedings of the IEEE/CVF conference on computer vision and pattern recognition*, pages 15630–15640, 2024. 1
- [36] Chuofan Ma, Yi Jiang, Jiannan Wu, Zehuan Yuan, and Xiaojuan Qi. Groma: Localized visual tokenization for grounding multimodal large language models. In *European Conference on Computer Vision*, pages 417–435. Springer, 2024. 1
- [37] Muhammad Maaz, Hanoona Rasheed, Salman Khan, and Fahad Shahbaz Khan. Video-chatgpt: Towards detailed video understanding via large vision and language models. In *Proceedings of the 62nd Annual Meeting of the Association for Computational Linguistics (ACL 2024)*, 2024. 9
- [38] Jesse Mu, Xiang Li, and Noah Goodman. Learning to compress prompts with gist tokens. *Advances in Neural Information Processing Systems*, 36:19327–19352, 2023. 8
- [39] OpenAI. Gpt-4v(ision) system card. Technical report, OpenAI, 2023. 1
- [40] Zhiliang Peng, Wenhui Wang, Li Dong, Yaru Hao, Shaohan Huang, Shuming Ma, Qixiang Ye, and Furu Wei. Grounding multimodal large language models to the world. In *The Twelfth International Conference on Learning Representations*, 2024. 1
- [41] Yuzhang Shang, Mu Cai, Bingxin Xu, Yong Jae Lee, and Yan Yan. Llava-prumerge: Adaptive token reduction for efficient large multimodal models. *arXiv preprint arXiv:2403.15388*, 2024. 8
- [42] Amanpreet Singh, Vivek Natarajan, Meet Shah, Yu Jiang, Xinlei Chen, Dhruv Batra, Devi Parikh, and Marcus Rohrbach. Towards vqa models that can read. In *Proceedings of the IEEE/CVF Conference on Computer Vision and Pattern Recognition*, pages 8317–8326, 2019. 3, 6, 7, 12, 14
- [43] Yutao Sun, Li Dong, Yi Zhu, Shaohan Huang, Wenhui Wang, Shuming Ma, Quanlu Zhang, Jianyong Wang, and Furu Wei. You only cache once: Decoder-decoder architectures for language models. *Advances in Neural Information Processing Systems*, 37:7339–7361, 2025. 8
- [44] Hugo Touvron, Louis Martin, Kevin Stone, Peter Albert, Amjad Almahairi, Yasmine Babaei, Nikolay Bashlykov, Soumya Batra, Prajjwal Bhargava, Shruti Bhosale, et al. Llama 2: Open foundation and fine-tuned chat models. *arXiv preprint arXiv:2307.09288*, 2023. 1
- [45] Pavan Kumar Anasalu Vasu, Fartash Faghri, Chun-Liang Li, Cem Koc, Nate True, Albert Antony, Gokul Santhanam, James Gabriel, Peter Grasch, Oncel Tuzel, et al. Fastvlm: Efficient vision encoding for vision language models. *arXiv preprint arXiv:2412.13303*, 2024. 8
- [46] Ashish Vaswani, Noam Shazeer, Niki Parmar, Jakob Uszkoreit, Llion Jones, Aidan N Gomez, Łukasz Kaiser, and Illia Polosukhin. Attention is all you need. In *Advances in Neural Information Processing Systems*, 2017. 1
- [47] Junyang Wang, Haiyang Xu, Jiabo Ye, Ming Yan, Weizhou Shen, Ji Zhang, Fei Huang, and Jitao Sang. Mobile-agent: Autonomous multi-modal mobile device agent with visual perception. *arXiv preprint arXiv:2401.16158*, 2024. 1
- [48] Qiong Wu, Wenhao Lin, Weihao Ye, Yiyi Zhou, Xiaoshuai Sun, and Rongrong Ji. Accelerating multimodal large language models via dynamic visual-token exit and the empirical findings. *arXiv preprint arXiv:2411.19628*, 2024. 8
- [49] Guangxuan Xiao, Yuandong Tian, Beidi Chen, Song Han, and Mike Lewis. Efficient streaming language models with attention sinks. In *The Twelfth International Conference on Learning Representations*, 2024. 8
- [50] Long Xing, Qidong Huang, Xiaoyi Dong, Jiajie Lu, Pan Zhang, Yuhang Zang, Yuhang Cao, Conghui He, Jiaqi Wang, Feng Wu, et al. Pyramiddrop: Accelerating your large vision-language models via pyramid visual redundancy reduction. *arXiv preprint arXiv:2410.17247*, 2024. 5, 6, 8, 11
- [51] Dejing Xu, Zhou Zhao, Jun Xiao, Fei Wu, Hanwang Zhang, Xiangnan He, and Yueting Zhuang. Video question answering via gradually refined attention over appearance and motion. In *Proceedings of the ACM international conference on Multimedia*, pages 1645–1653, 2017. 6, 14
- [52] Senqiao Yang, Yukang Chen, Zhuotao Tian, Chengyao Wang, Jingyao Li, Bei Yu, and Jiaya Jia. Visionzip: Longer is better but not necessary in vision language models. *arXiv preprint arXiv:2412.04467*, 2024. 2, 5, 6, 8, 10, 11, 12
- [53] Yuan Yao, Tianyu Yu, Ao Zhang, Chongyi Wang, Junbo Cui, Hongji Zhu, Tianchi Cai, Haoyu Li, Weilin Zhao, Zhihui He, et al. Minicpm-v: A gpt-4v level mllm on your phone. *arXiv preprint arXiv:2408.01800*, 2024. 1
- [54] Jiabo Ye, Anwen Hu, Haiyang Xu, Qinghao Ye, Ming Yan, Yuhao Dan, Chenlin Zhao, Guohai Xu, Chenliang Li, Junfeng Tian, et al. mplug-docowl: Modularized multimodal large language model for document understanding. *arXiv preprint arXiv:2307.02499*, 2023. 1
- [55] Weihao Ye, Qiong Wu, Wenhao Lin, and Yiyi Zhou. Fit and prune: Fast and training-free visual token pruning for multi-modal large language models. *arXiv preprint arXiv:2409.10197*, 2024. 8
- [56] Xubing Ye, Yukang Gan, Yixiao Ge, Xiao-Ping Zhang, and Yansong Tang. Atp-llava: Adaptive token pruning for large vision language models. *arXiv preprint arXiv:2412.00447*, 2024. 8
- [57] Weihao Yu, Zhengyuan Yang, Linjie Li, Jianfeng Wang, Kevin Lin, Zicheng Liu, Xinchao Wang, and Lijuan Wang. Mm-vet: Evaluating large multimodal models for integrated capabilities. *arXiv preprint arXiv:2308.02490*, 2023. 7, 13, 14

- [58] Zhou Yu, Dejing Xu, Jun Yu, Ting Yu, Zhou Zhao, Yueting Zhuang, and Dacheng Tao. Activitynet-qa: A dataset for understanding complex web videos via question answering. In *AAAI*, pages 9127–9134, 2019. [6](#), [14](#)
- [59] Xiang Yue, Yuansheng Ni, Kai Zhang, Tianyu Zheng, Ruoqi Liu, Ge Zhang, Samuel Stevens, Dongfu Jiang, Weiming Ren, Yuxuan Sun, et al. Mmmu: A massive multi-discipline multimodal understanding and reasoning benchmark for expert agi. In *Proceedings of the IEEE/CVF Conference on Computer Vision and Pattern Recognition*, pages 9556–9567, 2024. [14](#)
- [60] Chi Zhang, Zhao Yang, Jiakuan Liu, Yucheng Han, Xin Chen, Zebiao Huang, Bin Fu, and Gang Yu. Appagent: Multimodal agents as smartphone users. *arXiv preprint arXiv:2312.13771*, 2023. [1](#)
- [61] Qizhe Zhang, Aosong Cheng, Ming Lu, Zhiyong Zhuo, Minqi Wang, Jiajun Cao, Shaobo Guo, Qi She, and Shanghang Zhang. [cls] attention is all you need for training-free visual token pruning: Make vlm inference faster. *arXiv preprint arXiv:2412.01818*, 2024. [2](#), [6](#), [8](#), [11](#)
- [62] Yuan Zhang, Chun-Kai Fan, Junpeng Ma, Wenzhao Zheng, Tao Huang, Kuan Cheng, Denis Gudovskiy, Tomoyuki Okuno, Yohei Nakata, Kurt Keutzer, et al. Sparsevlm: Visual token sparsification for efficient vision-language model inference. *arXiv preprint arXiv:2410.04417*, 2024. [2](#), [3](#), [5](#), [6](#), [8](#), [11](#)
- [63] Zhenyu Zhang, Ying Sheng, Tianyi Zhou, Tianlong Chen, Lianmin Zheng, Ruisi Cai, Zhao Song, Yuandong Tian, Christopher Ré, Clark Barrett, et al. H2o: Heavy-hitter oracle for efficient generative inference of large language models. *Advances in Neural Information Processing Systems*, 36: 34661–34710, 2023. [8](#)
- [64] Zeliang Zhang, Phu Pham, Wentian Zhao, Kun Wan, Yu-Jhe Li, Jianing Zhou, Daniel Miranda, Ajinkya Kale, and Chenliang Xu. Treat visual tokens as text? but your mllm only needs fewer efforts to see. *arXiv preprint arXiv:2410.06169*, 2024. [5](#), [8](#)
- [65] Zhi Zhang, Srishti Yadav, Fengze Han, and Ekaterina Shutova. Cross-modal information flow in multimodal large language models. *arXiv preprint arXiv:2411.18620*, 2024. [5](#), [8](#)
- [66] Wangbo Zhao, Yizeng Han, Jiasheng Tang, Zhikai Li, Yibing Song, Kai Wang, Zhangyang Wang, and Yang You. A stitch in time saves nine: Small vlm is a precise guidance for accelerating large vlms. *arXiv preprint arXiv:2412.03324*, 2024. [8](#)
- [67] Zixuan Zhou, Xuefei Ning, Ke Hong, Tianyu Fu, Jiaming Xu, Shiyao Li, Yuming Lou, Luning Wang, Zhihang Yuan, Xiuhong Li, et al. A survey on efficient inference for large language models. *arXiv preprint arXiv:2404.14294*, 2024. [2](#)
- [68] Deyao Zhu, Jun Chen, Xiaoqian Shen, Xiang Li, and Mohamed Elhoseiny. MiniGPT-4: Enhancing vision-language understanding with advanced large language models. In *The Twelfth International Conference on Learning Representations*, 2024. [1](#)